Draft version September 26, 2014
Preprint typeset using LaTeX style emulateapj v. 5/2/11

NUCLEOSYNTHESIS CONSTRAINTS ON THE NEUTRON STAR-BLACK HOLE MERGER RATE

A. Bauswein[1], R. Ardevol Pulpillo[2,3], H.-T. Janka[2], and S. Goriely[4]

Draft version September 26, 2014

ABSTRACT

We derive constraints on the time-averaged event rate of neutron star-black hole (NS-BH) mergers by using estimates of the population-integrated production of heavy rapid neutron-capture (r-process) elements with nuclear mass numbers $A > 140$ by such events in comparison to the Galactic repository of these chemical species. Our estimates are based on relativistic hydrodynamical simulations convolved with theoretical predictions of the binary population. This allows us to determine a strict upper limit of the average NS-BH merger rate of $\sim 6\times10^{-5}$ per year. We quantify the uncertainties of this estimate to be within factors of a few mostly because of the unknown BH spin distribution of such systems, the uncertain equation of state of NS matter, and possible errors in the Galactic content of r-process material. Our approach implies a correlation between the merger rates of NS-BH binaries and of double NS systems. Predictions of the detection rate of gravitational-wave signals from such compact-object binaries by Advanced LIGO and Advanced Virgo on the optimistic side are incompatible with the constraints set by our analysis.

Subject headings: gravitational waves — hydrodynamics — nuclear reactions, nucleosynthesis, abundances — black hole physics — stars: neutron — binaries: close

1. INTRODUCTION

To date no neutron star-black hole (NS-BH) binaries are known. Such compact object binaries, however, emit gravitational-waves (GWs), which for some systems leads to the merging of the binary components within the Hubble time. The inspiral and coalescence of NS-BH and NS-NS binaries are among the primary targets for the upcoming Advanced LIGO and Advanced Virgo GW detectors (Abadie et al. 2010). Compact object mergers (COMs) that lead to a post-merging accretion torus around the relic BH are also promising progenitor candidates of short-hard gamma-ray bursts (GRBs) (Paczynski 1986; Eichler et al. 1989; Berger 2014). Some fraction of the stellar matter is expected to become gravitationally unbound during and after the binary collision and is likely to undergo the rapid neutron-capture process (r-process) (Lattimer & Schramm 1974; Lattimer et al. 1977), creating neutron-rich elements whose astrophysical production site has not been unambiguously identified yet. Evidence from chemogalactic evolution studies grows that COMs could be the dominant sources of the Galactic heavy r-process nuclei (traced by the enrichment history of europium; Mennekens & Vanbeveren 2014; Shen et al. 2014; van de Voort et al. 2014, and references therein). The radioactive decays of r-process material may power the thermal emission of a detectable electromagnetic counterpart of the merger (Li & Paczyński 1998; Metzger et al. 2010). Tentative evidence for such an event has been reported by Berger et al. (2013); Tanvir et al. (2013).

[1] Department of Physics, Aristotle University of Thessaloniki, GR-54124 Thessaloniki, Greece
[2] Max Planck Institute for Astrophysics, Karl-Schwarzschild-Str. 1, 85748 Garching, Germany
[3] Physik Department, Technische Universität München, James-Franck-Str. 1, 85748 Garching, Germany
[4] Institut d'Astronomie et d'Astrophysique, Université Libre de Bruxelles, C.P. 226, B-1050 Brussels, Belgium

Because of the lack of observational data, predictions of the frequency of NS-BH mergers rely on theoretical studies (e.g. Tutukov & Yungelson 1993; Voss & Tauris 2003; O'Shaughnessy et al. 2008; Dominik et al. 2012; Mennekens & Vanbeveren 2014; Dominik et al. 2013; Postnov & Yungelson 2014). These population synthesis models estimate Galactic merger rates between 2×10^{-9} and 10^{-5} per year (Postnov & Yungelson 2014). The range reflects the challenge in comprehensively modelling the formation and evolution of stellar binaries and their remnants.

In this work we determine an independent upper limit on the merger rate of NS-BH binaries by comparing the predicted r-process nucleosynthesis yields of such systems with the observed Galactic amount of r-process material. Similar arguments were used, e.g., in Lattimer & Schramm (1974); Freiburghaus et al. (1999); Qian (2000); Metzger et al. (2010); Goriely et al. (2011); Korobkin et al. (2012); Rosswog et al. (2013); Bauswein et al. (2013); Piran et al. (2014) mostly in the context of NS-NS mergers or COMs in general. Here we elaborate on these estimates by employing population integrated yields, which is crucial for NS-BH systems because of the strong dependence on binary parameters. We use ejecta masses determined by relativistic simulations of relevant NS-BH systems and, in particular, quantify the uncertainties of our estimates. Information on the hydrodynamical and nucleosynthesis calculations of NS-BH systems is provided in Sect. 2. Our rate estimates are discussed in Sect. 3 and combined with NS-NS mergers in Sect. 4. We finish with conclusions in Sect. 5.

2. NUMERICAL MODELING

We simulate NS-BH mergers with a relativistic smooth particle hydrodynamics (SPH) code, which evolves the hydrodynamical quantities comoving with the fluid (Oechslin et al. 2002; Bauswein 2010; Just et al. 2014). The Einstein equations are solved by imposing the conformal flatness condition (CFC) on the spatial metric as

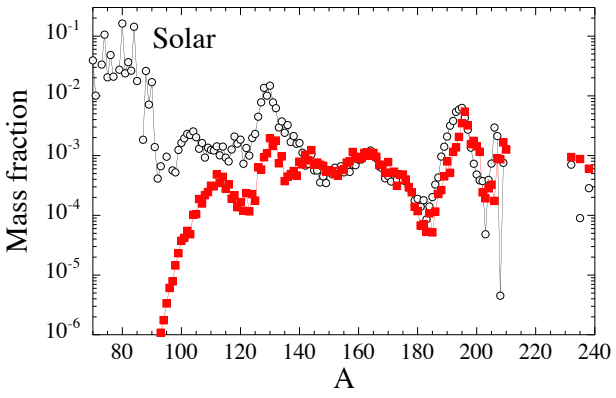

FIG. 1.— Abundance distribution vs. atomic mass for merger ejecta of a $1.35\,M_\odot$ NS and a $7\,M_\odot$ BH with $a_{\rm BH} = 0.5$ (red symbols) normalised to the solar distribution (black symbols; normalized to unity) in the $A = 165$ rare-earth region.

formulated in Cordero-Carrión et al. (2009). This allows us to model the spinning and moving BH by the "static puncture" approach (Brandt & Brügmann 1997), which is commonly used to construct initial data for fully relativistic calculations (Shibata & Taniguchi 2011). (Despite the term "static puncture" the BH carries linear and angular momentum and moves during the simulations (Bauswein 2010; Shibata & Taniguchi 2011).) To this end we replace the metric equations in our hydrodynamics solver of Oechslin et al. (2002) by Eqs. (59)–(62) of Shibata & Taniguchi (2011), using their definitions of Eqs. (56)–(58) for treating BH spin and momentum. Our existing multigrid solver then yields the metric for NS-BH systems within the CFC approximation.

The simulations start from circular quasi-equilibrium orbits a few revolutions before merging. The NSs are initially nonrotating, while we investigate different initial BH spins perpendicular to the orbital plane. The NS matter is initially at zero temperature and in neutrinoless beta-equilibrium. We employ the microphysical DD2 equation of state (EoS) (Hempel & Schaffner-Bielich 2010), which is a moderately stiff EoS and yields a NS radius of 13.21 km for a $1.35\,M_\odot$ NS. The fluid is modelled with a resolution of ∼170,000 SPH particles. We test different resolutions to confirm that our results are converged, in particular the ejecta mass is determined with an accuracy of ∼30%.

Throughout this paper we quantify the (initial) BH spin by the dimensionless spin parameter $a_{\rm BH} = J_{\rm BH}/M_{\rm BH}^2$ with the BH angular momentum $J_{\rm BH}$ and gravitational mass $M_{\rm BH}$. Masses refer to the gravitational mass of the object (for binaries at infinite separation).

For fixed NS mass of $M_{\rm NS} = 1.35\ M_\odot$ we compute the ejecta masses for systems with initial BH masses of 5, 7, and $10\,M_\odot$ and initial BH spins varied between 0.0 and 0.9 (see Table 1). The initial spin $a_{\rm BH}$ has the strongest impact on the ejecta mass. For $M_{\rm BH} = 5\,M_\odot$ $M_{\rm ej}$ grows by a factor of ∼200 when $a_{\rm BH}$ is increased from zero to 0.9. For systems with the same $a_{\rm BH}$, the ejecta mass shows only a moderate variation with increasing $M_{\rm BH}$ until $M_{\rm ej}$ starts to plummet at higher BH masses. This behavior is understandable because

TABLE 1
EJECTA MASSES

$a_{\rm BH}$ \ $M_{\rm BH}$	$5\ M_\odot$	$7\ M_\odot$	$10\ M_\odot$
0	$0.0004\ M_\odot$	$\lesssim 2\times10^{-6}\ M_\odot$	$\lesssim 2\times10^{-6}\ M_\odot$
0.5	$0.042\ M_\odot$	$0.0090\ M_\odot$	$0.0018\ M_\odot$
0.7	$0.067\ M_\odot$	$0.070\ M_\odot$	$0.073\ M_\odot$
0.9	$0.096\ M_\odot$	$0.087\ M_\odot$	$0.086\ M_\odot$

NOTE. — NS-BH mergers with initial BH mass $M_{\rm BH}$, initial BH spin $a_{\rm BH}$, NS mass $1.35\ M_\odot$, and DD2 EoS.

with increasing $M_{\rm BH}$ the radius of the innermost stable orbit grows faster than the tidal disruption radius until the tidal disruption of the NS changes to a plunge at higher $M_{\rm BH}$. The steep reduction of $M_{\rm ej}$ occurs at higher BH mass for higher initial spin. Our results are qualitatively and quantitatively consistent with the findings of Hotokezaka et al. (2013); Foucart et al. (2013); Kyutoku et al. (2013); Foucart et al. (2014). For instance in Kyutoku et al. (2013), a sequence with fixed $a_{\rm BH}$ of 0.75 yields ejecta masses of 0.04–$0.05\,M_\odot$ for BH masses between 4.05 and $9.45\,M_\odot$ with the H4 EoS. The ejecta masses agree very well with our results for the DD2 EoS, which yields NS radii comparable to those of the H4 EoS. The simulations of Foucart et al. (2014) with a somewhat softer EoS (LS220) find ejecta masses between $\sim0.04\,M_\odot$ and $\sim0.15\,M_\odot$ for systems involving BHs with spins $a_{\rm BH} = 0.7$–0.9 and NSs with $M_{\rm NS} = 1.2$–$1.4\ M_\odot$, again in very good agreement with our computations.

Following Goriely et al. (2011) we perform nucleosynthesis calculations for a selected subset of models (detailed paper in preparation). About 75% of the ejecta produce heavy r-process elements with mass numbers $A \gtrsim 140$ in close similarity to the solar r-process abundance distribution (Fig. 1).

3. RATE ESTIMATES

The Galactic r-process material is estimated from the total Galactic baryon mass, $M_{\rm Gal} \simeq 6\times10^{10}\ M_\odot$ (McMillan 2011), and the solar system r-process mass fraction, assuming the latter is representative for the whole Galaxy (as suggested by the small scatter of the europium abundance in the present-day Milky Way). Here, we only consider r-process elements with $A > 140$, which can be produced significantly by NS-BH mergers and in proportions close to the solar abundances (cf. Fig. 1). Including elements with $A < 140$ would require to add the contribution from the NS-BH merger remnants and would increase the uncertainties in the total ejecta mass (see Just et al. 2014).

Decomposing the solar-system abundances of elements heavier than iron into their s- and r-process components (Goriely 1999), the total mass fraction of r-process elements with $A > 140$ in the solar system is estimated as $X^\odot_{r,A>140} = 3.1\times10^{-8}$. This implies a Galactic content of such material of $\sim M_{r,A>140} = M_{\rm Gal}\times X^\odot_{r,A>140} = 1860\ M_\odot$.

The r-process inventory of $M_{r,A>140}$ has to be compared with the yield of $A > 140$ material (75% of the total ejecta) from the NS-BH population over the Galactic history of $T_{\rm Gal} = 10^{10}$ yrs. We estimate the production by NS-BH mergers by convolving the ejecta mass in dependence on the binary parameters with the binary distribution provided by population synthesis or deduced

from observations.

Depending on the metallicity and other model assumptions, population synthesis studies by Dominik et al. (2012)[5] predict average BH masses of 8–10 $M_\odot$, roughly consistent with observations (McClintock et al. 2013). For simplicity and independence of additional modeling assumptions (like delay-time distribution and metallicity evolution), we consider only the time-averaged merger rate over the Galactic history. We exclude binaries with lifetimes exceeding the age of the Galaxy and checked that our estimates do not depend significantly on the lifetimes of the merging systems. Our constraints yield firm upper limits of the present-day NS-BH merger rate.

The merging binaries contain NSs with an average mass of about 1.5 $M_\odot$, while for computational reasons and for a better comparison with the literature we employ a NS mass of 1.35 $M_\odot$ compatible with earlier population synthesis models (Belczynski et al. 2008) and NS masses observed in double NS binaries (Özel et al. 2012). This assumption may introduce an uncertainty of a factor of two (Foucart et al. 2014). The distribution of BH spins is not available from the adopted population synthesis models. Hence, we treat the average BH spin as a free parameter. The BH spin may be misaligned with the rotation axis of the binary. About 30–80% of the binaries might have misalignments >30° (Kalogera 2000). Rantsiou et al. (2008) showed that for tilts below 30° the ejecta mass is practically identical to the aligned case, whereas the ejecta vanish for tilt angles exceeding 45°. Here we adopt a fraction $f_{\rm tilt} = 0.5$ of binaries with tilts sufficiently small to eject matter as the aligned case. The remaining fraction of systems is assumed to yield no ejecta. Our value of $f_{\rm tilt}$ is compatible with findings of Belczynski et al. (2008), and $f_{\rm tilt}$ is expected to vary at most between 0.2 and 0.8.

Using these assumptions the upper limit on the NS-BH merger rate is estimated by

$$R_{\rm NSBH} = \frac{M_{r,A>140}}{0.75\widetilde{M}_{\rm ej}(a_{\rm BH})T_{\rm Gal}f_{\rm tilt}}. \quad (1)$$

$\widetilde{M}_{\rm ej}$ denotes the population averaged ejecta mass per merger event multiplied by 0.75 to consider only ejecta with $A > 140$. Figure 2 shows the rate as function of $a_{\rm BH}$ (solid line) for the standard model of Dominik et al. (2012) (their "submodel" A) at 1/10 solar metallicity, where most of the mergers are expected to take place (Dominik et al. 2013). We find a strong BH spin dependence. For slowly spinning BHs with $a_{\rm BH} = 0.1$ the merger rate can be as high as $2.7 \times 10^{-4}\,{\rm yr}^{-1}$, whereas rapid rotation with $a_{\rm BH} = 0.9$ results in a much lower rate of $3.6 \times 10^{-6}\,{\rm yr}^{-1}$.

The BH spin is likely to be considerably higher than 0.1 because it is determined by the initial spin after the supernova and the subsequent accretion in the binary system. In O'Shaughnessy et al. (2005) mass transfer in binaries was found to be strong and thus to lead to generally high spins between 0.4 and 0.9 and spin-orbit alignment. In Belczynski et al. (2008) the accretion during the binary evolution increases the initial BH spin only moderately implying that the initial spin is the most important parameter. Observations of X-ray binaries suggest that most BHs have spin parameters exceeding 0.5 with an average $a_{\rm BH}$ of ∼0.6 (McClintock et al. 2013). These spins correspond to upper limits of the NS-BH merger rate of $\sim 6 \times 10^{-5}\,{\rm yr}^{-1}$ and $8 \times 10^{-6}\,{\rm yr}^{-1}$, respectively. The latter value is roughly compatible with the rate of of $3.4 \times 10^{-6}\,{\rm yr}^{-1}$ predicted by the standard model of Dominik et al. (2012).

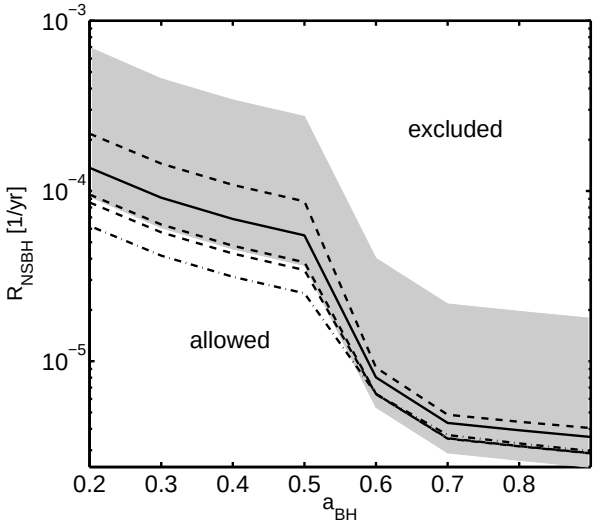

FIG. 2.— Upper limit on the Galactic NS-BH merger rate as function of BH spin for different population synthesis models of Dominik et al. (2012). The solid line corresponds to their standard model ("submodel A" at 1/10 solar metallicity). Dashed lines show variations to the standard model. The shaded region indicates uncertainties because of the unknown NS EoS. A rate estimate entirely based on the observed BH mass distribution is given by the dash-dotted line.

For $M_{\rm BH}/M_{\rm NS} = 3$ Kyutoku et al. (2013) and Hotokezaka et al. (2013) showed that for soft (stiff) EoSs the ejecta masses can be a factor 5 lower (1.5 higher) compared to those for the H4 EoS, which is similar to our DD2 EoS. The corresponding range of uncertainty is indicated by grey shading in Fig. 2. This variation is consistent with the EoS effects quantified for ideal fluid EoSs by Foucart et al. (2013) for another binary setup. The relatively high ejecta masses found by Foucart et al. (2014) for the soft LS220 EoS suggest that a factor of 5 might overestimate changes associated with very soft EoSs. Moreover, theoretical arguments favor a nuclear EoS comparable to or slightly softer than DD2 (Hebeler et al. 2013).

Variants of the standard model of Dominik et al. (2012) for different metallicities (e.g., dashed lines in Fig. 2 for solar metallicity and/or "submodel" B) yield NS-BH merger rates between $2.4 \times 10^{-5}\,{\rm yr}^{-1}$ and $8.7 \times 10^{-5}\,{\rm yr}^{-1}$ for $a_{\rm BH} = 0.5$. The dash-dotted line in Fig. 2 provides a rate limit independent of population synthesis studies by using the observed BH mass distribution of Özel et al. (2012) with a median at 7.5 $M_\odot$. Because of the lower mean BH mass, this case yields slightly lower rates than the population models. Again, for an average $a_{\rm BH}$ >0.5 this rate limit is roughly compatible with the merger rate derived from population synthesis at 1/10 solar metallicity (Dominik et al. 2012).

4. CONSTRAINTS FROM NS-NS BINARIES

[5] www.syntheticuniverse.org

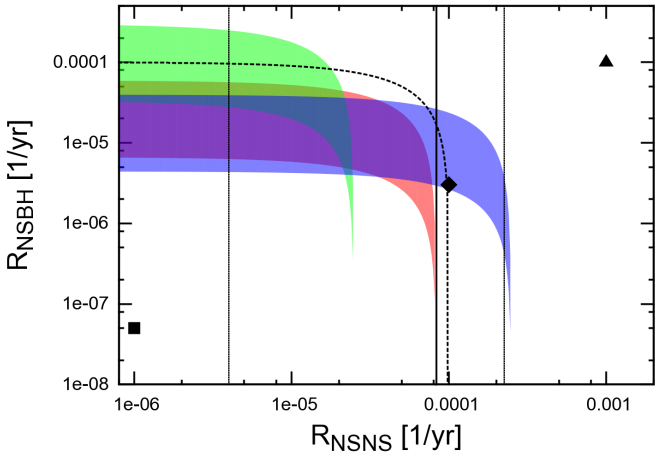

FIG. 3.— Average Galactic NS-BH merger rate vs. NS-NS merger rate for the DD2 EoS (reddish band), a stiff EoS (bluish band), and a soft EoS (greenish band). The widths of the bands represent variations with average BH spins between 0.5 and 0.7. Symbols indicate "optimistic" (triangle), "realistic" (diamond) and "pessimistic" (square) merger rates as compiled in Abadie et al. (2010). Vertical lines mark NS-NS merger rates inferred from binary NS observations with uncertainty range (Kalogera et al. 2004). The dashed line approximates a rate estimate derived from observed GRBs (Berger 2014).

Most population models predict NS-NS mergers to be more frequent than NS-BH collisions (Postnov & Yungelson 2014). The average ejecta mass of NS-NS mergers depends strongly on the high-density EoS and is typically smaller than that of NS-BH mergers. In contrast to NS-BH mergers, double NS collisions produce more ejecta for soft EoSs (Bauswein et al. 2013; Hotokezaka et al. 2013). In this case the population averaged ejecta mass may be $\widetilde{M}_{\rm ej,NSNS} \approx 10^{-2}\,M_\odot$, whereas stiff EoSs lead to $\widetilde{M}_{\rm ej,NSNS} \approx 10^{-3}\,M_\odot$; for the DD2 EoS $\widetilde{M}_{\rm ej,NSNS}$ amounts to $\sim 3\times10^{-3}\ M_\odot$ (Bauswein et al. 2013).

Quantifying the contribution from NS-NS mergers by a time-averaged merger rate $R_{\rm NSNS}$, the upper limit on the average Galactic rate for NS-BH mergers reads

$$R_{\rm NSBH} = \frac{M_{r,A>140} - 0.75\widetilde{M}_{\rm ej,NSNS} T_{\rm Gal} R_{\rm NSNS}}{0.75\widetilde{M}_{\rm ej}(a_{\rm BH}) T_{\rm Gal} f_{\rm tilt}}. \quad (2)$$

Here we also assume that 75% of the NS-NS merger ejecta form $A > 140$ nuclei (but see Wanajo et al. 2014, for possible corrections). The reddish band in Fig. 3 shows this relation between the two rates for our standard model (DD2, $f_{\rm tilt} = 0.5$) and an average $a_{\rm BH}$ between 0.5 and 0.7. The two merger rates are anti-correlated: higher contributions from NS-NS mergers reduce the ones from NS-BH mergers and vice versa. Such an anti-correlation also holds for different EoSs but with distinct shifts because of the opposite dependences of $\widetilde{M}_{\rm ej,NSNS}$ and $\widetilde{M}_{\rm ej}$ on the stiffness of the EoS. For very soft EoSs (greenish band) $\widetilde{M}_{\rm ej}$ may be reduced by at most a factor five relative to the DD2 case, whereas $M_{\rm ej,NSNS}$ should be $\sim 10^{-2}\,M_\odot$. If NS-BH mergers dominate, their rate limit is correspondingly higher, while for NS-NS binaries as main source the relatively large ejecta mass per event leads to tighter rate constraints. The opposite trends apply for stiff EoSs (bluish band), which yield stronger limits for $R_{\rm NSBH}$ but allow for more NS-NS coalescences. The intermediate (reddish) case implies that NS-NS mergers as additional r-process source set a strict upper bound of $\sim 6\times10^{-5}\,{\rm yr}^{-1}$ for the NS-BH merger rate. The bluish and greenish bands represent rather extreme EoS variations.

The symbols in Fig. 3 display "pessimistic" (square), "realistic" (diamond) and "optimistic" (triangle) merger rates of both event types as compiled in Abadie et al. (2010) to estimate the GW detection probability by Advanced LIGO and Advanced Virgo. The "optimistic" case is practically ruled out by our estimates because already NS-BH or NS-NS mergers alone would overproduce r-process nuclei. The "realistic" expectations for NS-NS and NS-BH detection rates (diamond) are marginally consistent with our constraints.

The vertical solid line in Fig. 3 marks $R_{\rm NSBH}$ derived from the observed binary NS population (Kalogera et al. 2004) with thin vertical lines indicating the corresponding uncertainties. Only very stiff EoSs allow for a substantial NS-BH merger rate that is clearly compatible with the observed double-NS population. The thick dashed line shows the sum $R_{\rm NSBH} + R_{\rm NSNS} = 10^{-4}\,{\rm yr}^{-1}$, which roughly corresponds to a volumetric rate of $10^3\,{\rm Gpc}^{-3}{\rm yr}^{-1}$ derived from the observed short-GRB rate and inferred jet opening angles (Berger 2014). Here we use a crude conversion from the volumetric rate to a Galactic merger rate (Abadie et al. 2010) and assume that every NS-BH and NS-NS merger produces a beamed GRB. Giving up the latter assumption would result in a higher rate, i.e., a curve shifted to the upper right. Given the involved uncertainties the rate inferred from GRBs is roughly compatible with our estimates, which might be a hint that the far majority of COMs result in GRBs unless another, r-process inactive source contributes to making short GRBs.

Any rate estimates, e.g. by population synthesis models, should be checked for consistency with the correlation given by Eq. (2). For instance, considering the r-process yields of NS-NS mergers, the NS-BH merger rates of Dominik et al. (2012) are roughly compatible with our constraint. We emphasize that our time-averaged rates are upper limits of the current merger rate (e.g., Dominik et al. 2013; Mennekens & Vanbeveren 2014; Shen et al. 2014). Our rate constraints would even become more stringent if NS-NS and NS-BH mergers were not the only sources of $A > 140$ r-process elements (for suggestions, see, e.g., Arnould et al. 2007). While eccentric COMs with their higher ejecta masses (e.g. Rosswog et al. 2013) might occur with significant frequencies in dense stellar systems (Lee et al. 2010), additional ejecta from massive NSs and BH-torus systems as remnants of COMs (e.g. Fernández & Metzger 2013; Metzger & Fernández 2014; Perego et al. 2014; Just et al. 2014) are expected to contribute to the production of $A > 140$ r-nuclei only on a lower level (Just et al. 2014). Conversely, our bounds would be somewhat higher if COMs were less efficient in enriching the Galactic gas with r-elements, which might be suggested by the fact that 50% of the short GRBs exhibit projected offsets of >1.5 times the half-light radii of their host galaxies (Berger 2014).

5. SUMMARY AND OUTLOOK

We quantified an independent upper limit on the NS-BH merger rate, which, however, depends on the uncertain average BH spin. Adopting a moderately big spin parameter of $\gtrsim$0.5, the average merger rate should be $\lesssim 6 \times 10^{-5}\,\mathrm{yr}^{-1}$ with an uncertainty factor of a few. We point out that the NS-BH merger rate is correlated with the NS-NS coalescence rate, and population synthesis models should be checked for consistency with our combined constraint. The GW detection rates classified as "optimistic" ("realistic") for Advanced LIGO and Virgo (Abadie et al. 2010) are incompatible (marginally consistent) with our estimates considering that we deduced time-averaged rates, which are probably higher than the current rate relevant for GW detections (Dominik et al. 2013; Mennekens & Vanbeveren 2014); but see Voss & Tauris (2003) for opposite trends. Our rate limits are also roughly consistent with the possibility that NS-NS and NS-BH mergers are the dominant sources of short GRBs.

For improving our estimates, relativistic NS-BH merger simulations are needed for larger sets of high-density EoSs, different NS masses and BH spin orientations. Instead of time-averaged rate constraints a time-dependent analysis is desirable, accounting for the Galactic metallicity evolution and a consistent treatment of the metallicity dependence of NS-NS and NS-BH populations. More observational data on BH spins and a better understanding of natal BH spins and the spin evolution would reduce uncertainties considerably.

We thank T. Tauris for discussions, M. Hempel for EoS tables, and M. Dominik and C. Belczynski for population synthesis data and advice. A.B. is Marie Curie Intra-European Fellow within the 7th European Community Framework Programme (IEF 331873). S.G is F.R.S.-FNRS Research Associate. This work was supported by DFG through grants SFB/TR7 and EXC-153. Computing resources were provided by RZG and LRZ Garching.

REFERENCES

Abadie, J., et al. 2010, Classical and Quantum Gravity, 27, 173001
Arnould, M., Goriely, S., & Takahashi, K. 2007, Phys. Rep., 450, 97
Bauswein, A. 2010 (PhD thesis, Technical University Munich), http://mediatum.ub.tum.de?id=966127
Bauswein, A., Goriely, S., & Janka, H.-T. 2013, ApJ, 773, 78
Belczynski, K., Taam, R. E., Rantsiou, E., & van der Sluys, M. 2008, ApJ, 682, 474
Berger, E. 2014, ARA&A, 52, 43
Berger, E., Fong, W., & Chornock, R. 2013, ApJ, 774, L23
Brandt, S., & Brügmann, B. 1997, Physical Review Letters, 78, 3606
Cordero-Carrión, I., Cerdá-Durán, P., Dimmelmeier, H., Jaramillo, J. L., Novak, J., & Gourgoulhon, E. 2009, Phys. Rev. D, 79, 024017
Dominik, M., Belczynski, K., Fryer, C., Holz, D. E., Berti, E., Bulik, T., Mandel, I., & O'Shaughnessy, R. 2012, ApJ, 759, 52
—. 2013, ApJ, 779, 72
Eichler, D., Livio, M., Piran, T., & Schramm, D. N. 1989, Nature, 340, 126
Fernández, R., & Metzger, B. D. 2013, MNRAS, 435, 502
Foucart, F., et al. 2013, Phys. Rev. D, 87, 084006
—. 2014, Phys. Rev. D, 90, 024026
Freiburghaus, C., Rosswog, S., & Thielemann, F.-K. 1999, ApJ, 525, L121
Goriely, S. 1999, A&A, 342, 881
Goriely, S., Bauswein, A., & Janka, H.-T. 2011, ApJ, 738, L32
Hebeler, K., Lattimer, J. M., Pethick, C. J., & Schwenk, A. 2013, ApJ, 773, 11
Hempel, M., & Schaffner-Bielich, J. 2010, Nuclear Physics A, 837, 210
Hotokezaka, K., Kyutoku, K., Tanaka, M., Kiuchi, K., Sekiguchi, Y., Shibata, M., & Wanajo, S. 2013, ApJ, 778, L16
Just, O., Bauswein, A., Ardevol Pulpillo, R., Goriely, S., & Janka, H.-T. 2014, arXiv:1406.2687
Kalogera, V. 2000, ApJ, 541, 319
Kalogera, V., et al. 2004, ApJ, 614, L137
Korobkin, O., Rosswog, S., Arcones, A., & Winteler, C. 2012, MNRAS, 426, 1940
Kyutoku, K., Ioka, K., & Shibata, M. 2013, Phys. Rev. D, 88, 041503
Lattimer, J. M., Mackie, F., Ravenhall, D. G., & Schramm, D. N. 1977, ApJ, 213, 225
Lattimer, J. M., & Schramm, D. N. 1974, ApJ, 192, L145
Lee, W. H., Ramirez-Ruiz, E., & van de Ven, G. 2010, ApJ, 720, 953
Li, L.-X., & Paczyński, B. 1998, ApJ, 507, L59
McClintock, J. E., Narayan, R., & Steiner, J. F. 2013, Space Sci. Rev., in press (arXiv:1303.1583)
McMillan, P. J. 2011, MNRAS, 414, 2446
Mennekens, N., & Vanbeveren, D. 2014, A&A, 564, A134
Metzger, B. D., & Fernández, R. 2014, MNRAS, 441, 3444
Metzger, B. D., et al. 2010, MNRAS, 406, 2650
Oechslin, R., Rosswog, S., & Thielemann, F.-K. 2002, Phys. Rev. D, 65, 103005
O'Shaughnessy, R., Kaplan, J., Kalogera, V., & Belczynski, K. 2005, ApJ, 632, 1035
O'Shaughnessy, R., Kim, C., Kalogera, V., & Belczynski, K. 2008, ApJ, 672, 479
Özel, F., Psaltis, D., Narayan, R., & Santos Villarreal, A. 2012, ApJ, 757, 55
Paczynski, B. 1986, ApJ, 308, L43
Perego, A., Rosswog, S., Cabezon, R., Korobkin, O., Käppeli, R., Arcones, A., & Liebendörfer, M. 2014, MNRAS, 443, 3134
Piran, T., Korobkin, O., & Rosswog, S. 2014, arXiv:1401.2166
Postnov, K. A., & Yungelson, L. R. 2014, Living Rev. Rel., 17, 3
Qian, Y.-Z. 2000, ApJ, 534, L67
Rantsiou, E., Kobayashi, S., Laguna, P., & Rasio, F. A. 2008, ApJ, 680, 1326
Rosswog, S., Piran, T., & Nakar, E. 2013, MNRAS, 430, 2585
Shen, S., Cooke, R., Ramirez-Ruiz, E., Madau, P., Mayer, L., & Guedes, J. 2014, arXiv:1407.3796
Shibata, M., & Taniguchi, K. 2011, Living Reviews in Relativity, 14, 6
Tanvir, N. R., Levan, A. J., Fruchter, A. S., Hjorth, J., Hounsell, R. A., Wiersema, K., & Tunnicliffe, R. L. 2013, Nature, 500, 547
Tutukov, A. V., & Yungelson, L. R. 1993, Astronomy Reports, 37, 411
van de Voort, F., Quataert, E., Hopkins, P. F., Keres, D., & Faucher-Giguere, C.-A. 2014, arXiv:1407.7039
Voss, R., & Tauris, T. M. 2003, MNRAS, 342, 1169
Wanajo, S., Sekiguchi, Y., Nishimura, N., Kiuchi, K., Kyutoku, K., & Shibata, M. 2014, ApJ, 789, L39